

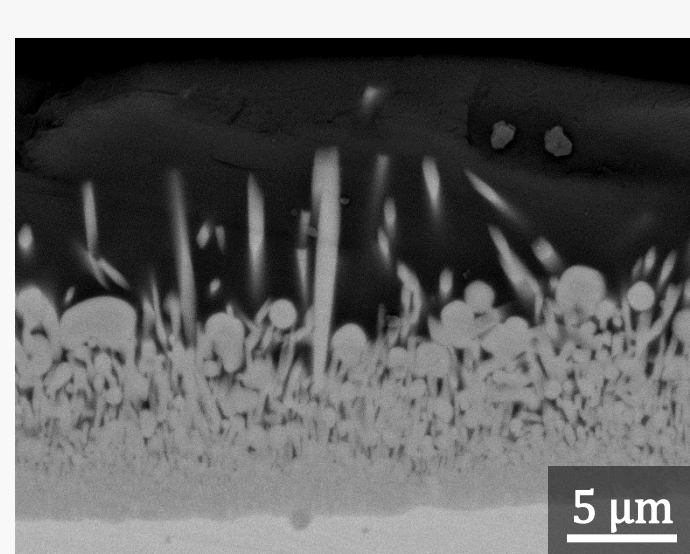
Jamesa L. Stokes<sup>1,2,4</sup>, Dr. Bryan J. Harder<sup>4</sup>, Dr. Valerie L. Wiesner<sup>4</sup>, Dr. Douglas E. Wolfe<sup>1,2,3</sup>

<sup>1</sup>Department of Materials Science and Engineering, <sup>2</sup>Applied Research Laboratory, <sup>3</sup>Department of Engineering Science and Mechanics, The Pennsylvania State University, University Park, PA 16802, USA, <sup>4</sup>NASA Glenn Research Center, Cleveland, OH 44135

## Objective

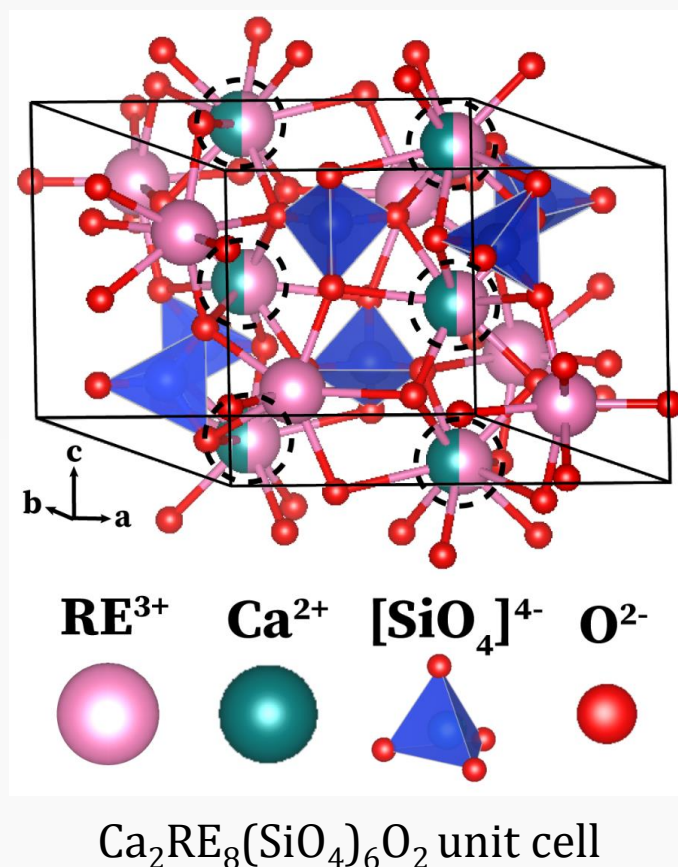
Rare earth (RE) disilicates are utilized in environmental barrier coatings (EBCs) to protect SiC-based ceramic matrix composites (CMCs) from destructive reactions with water vapor and other combustion species. These coating materials, however, degrade when exposed to molten silicate deposits primarily composed of calcium-magnesium aluminosilicates (CMAS). Coating materials are exposed to CMAS by engine ingestion of dust particulates from terrestrial sources during operation. Due to continual increases in engine operating temperature, it is important to understand the high temperature thermochemical mechanisms that drive corrosion of these materials. This work focuses on characterizing reaction products between disilicates and CMAS and optimizing coating chemistries to mitigate damage.

## Motivation and Background

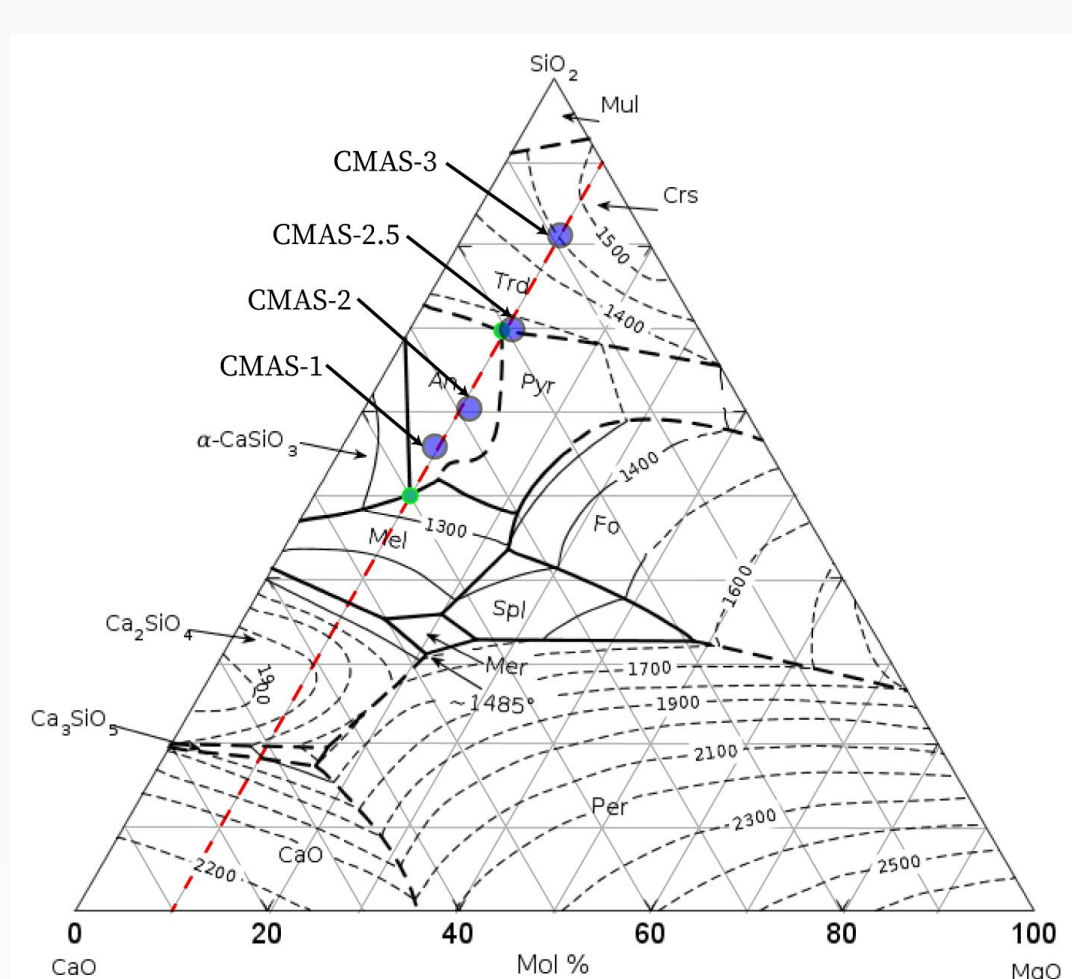


The use of coating materials with greater RE content promotes crystallization of the melt at coating surfaces.<sup>1</sup> A Ca-RE apatite type silicate is the most prominent phase in these interactions.

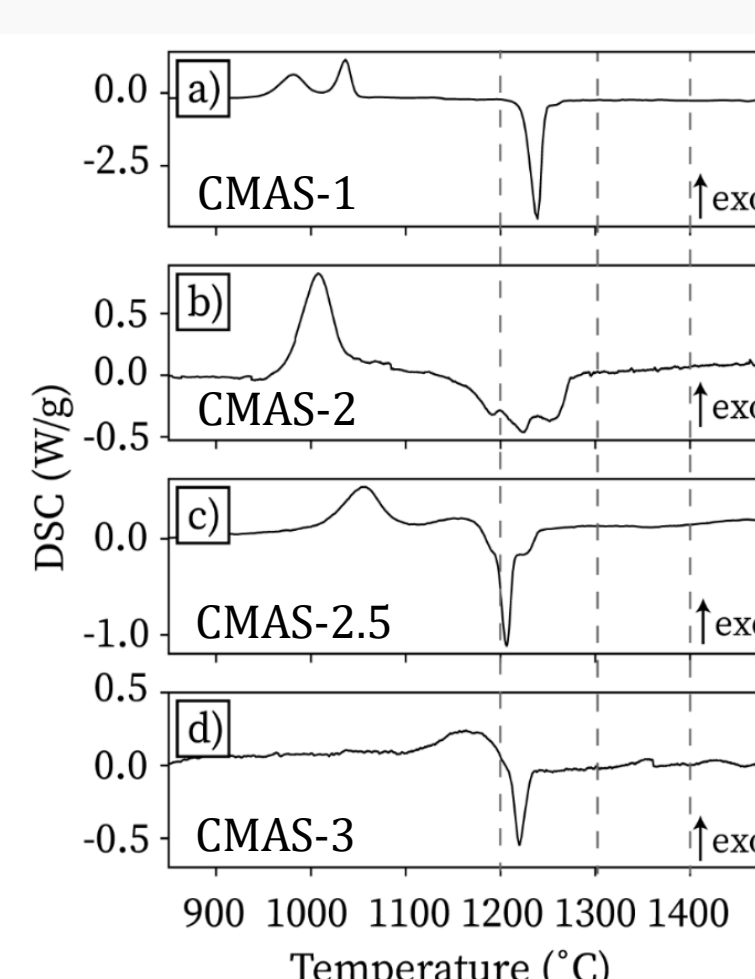
Recent studies demonstrated a decrease in apatite formation with ytterbium and yttrium disilicate as CaO content is decreased across CMAS melts. Studies on RE silicate crystal structures confirm metastability of apatite crystal structures with smaller RE cations.<sup>2</sup>



## CMAS Characterization



CaO-MgO-SiO<sub>2</sub> liquidus diagram at 15 wt% Al<sub>2</sub>O<sub>3</sub>.<sup>3</sup> The synthesized CMAS compositions are highlighted by the blue circles, and the MgO content line is highlighted in red.

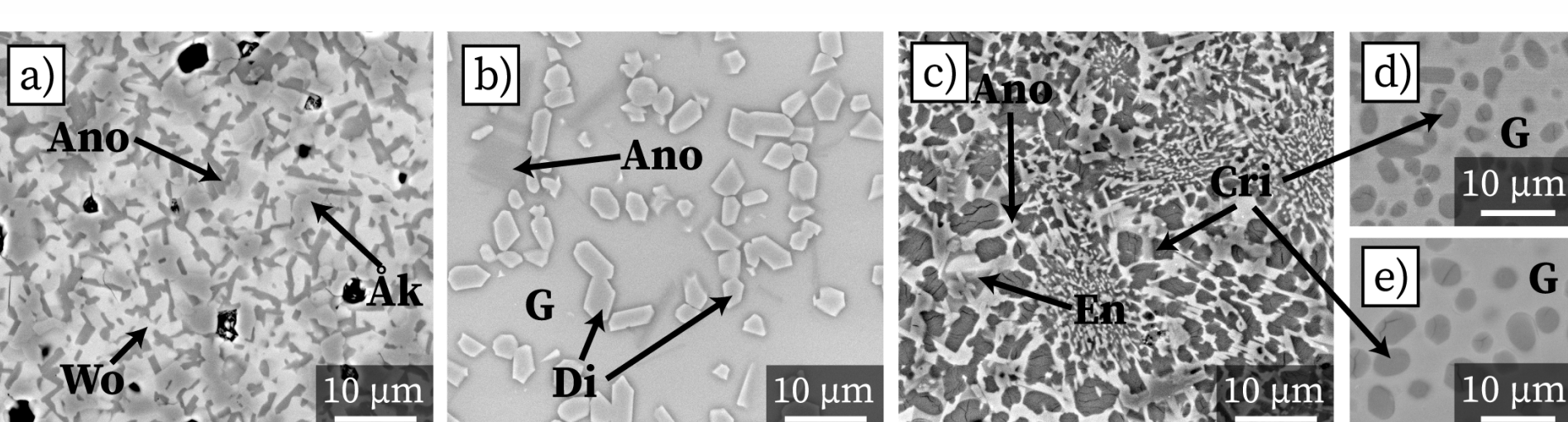


DSC scans of the CMAS compositions. The dashed lines indicate temperatures utilized for furnace heat treatments.

Four calcium-magnesium-aluminosilicate (CMAS) compositions were chosen based on relevancy to turbine engine operating environment. The Krämer<sup>1</sup> glass used in many investigations of coating materials with CMAS is also utilized in this study, which was originally formulated based on early studies of siliceous deposits in gas turbine engines (CMAS-1).<sup>4</sup> CaO:SiO<sub>2</sub> ratios of two additional CMAS compositions were determined from a desert sand composition previously investigated (CMAS-2)<sup>5</sup> and chemical analysis on 2010 Eyjafjallajökull volcanic ash (CMAS-3).

Compositions of synthesized CMAS glasses, determined by inductively coupled plasma atomic emission spectroscopy (ICP-AES).

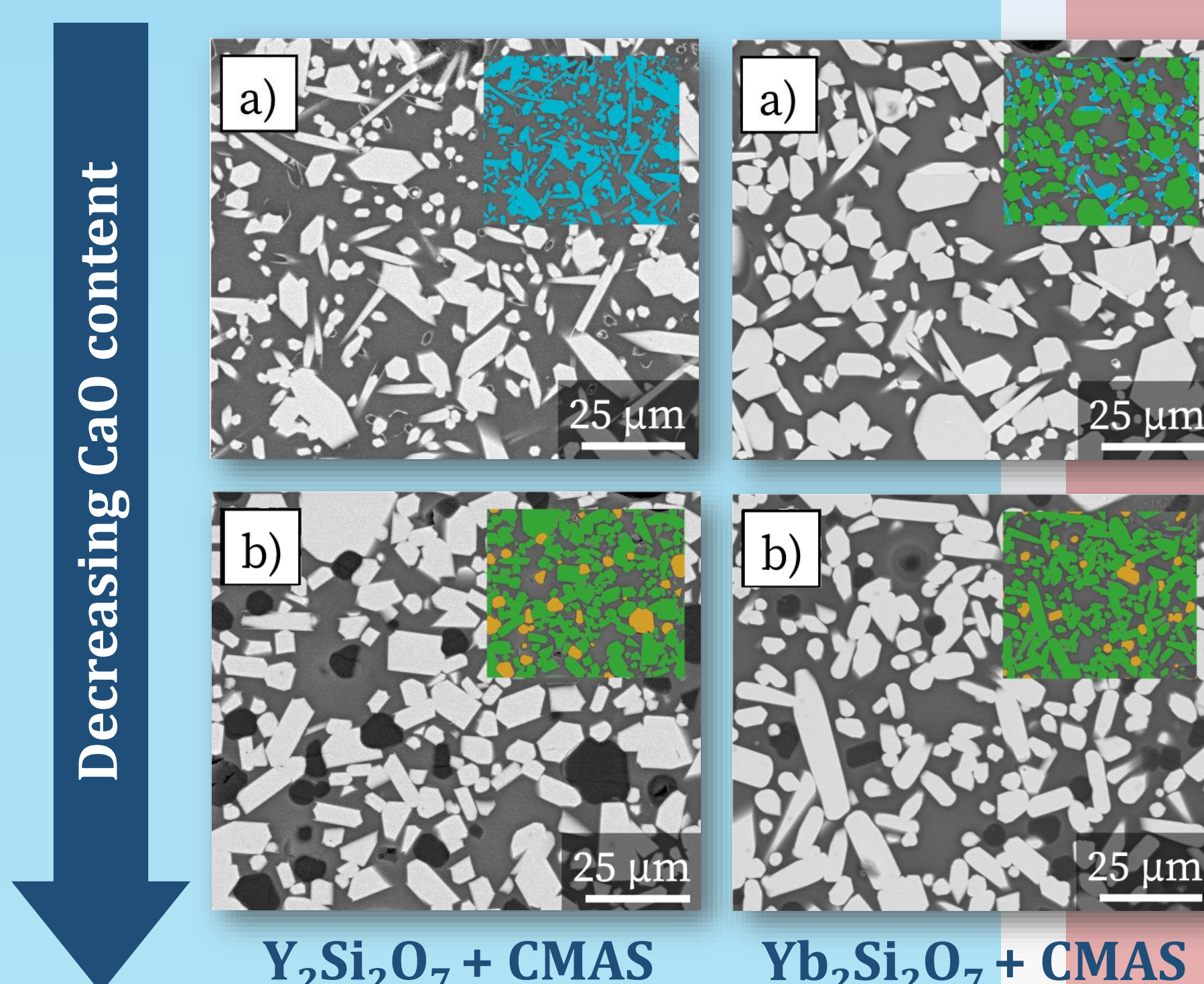
(mol%)	CMAS-1	CMAS-2	CMAS-2.5	CMAS-3
CaO	32.766	26.720	17.768	7.259
MgO	8.820	9.778	10.218	9.568
Al <sub>2</sub> O <sub>3</sub>	6.843	7.665	7.859	7.660
SiO <sub>2</sub>	51.571	55.836	64.155	75.512
CaO:SiO <sub>2</sub>	0.635	0.479	0.277	0.096



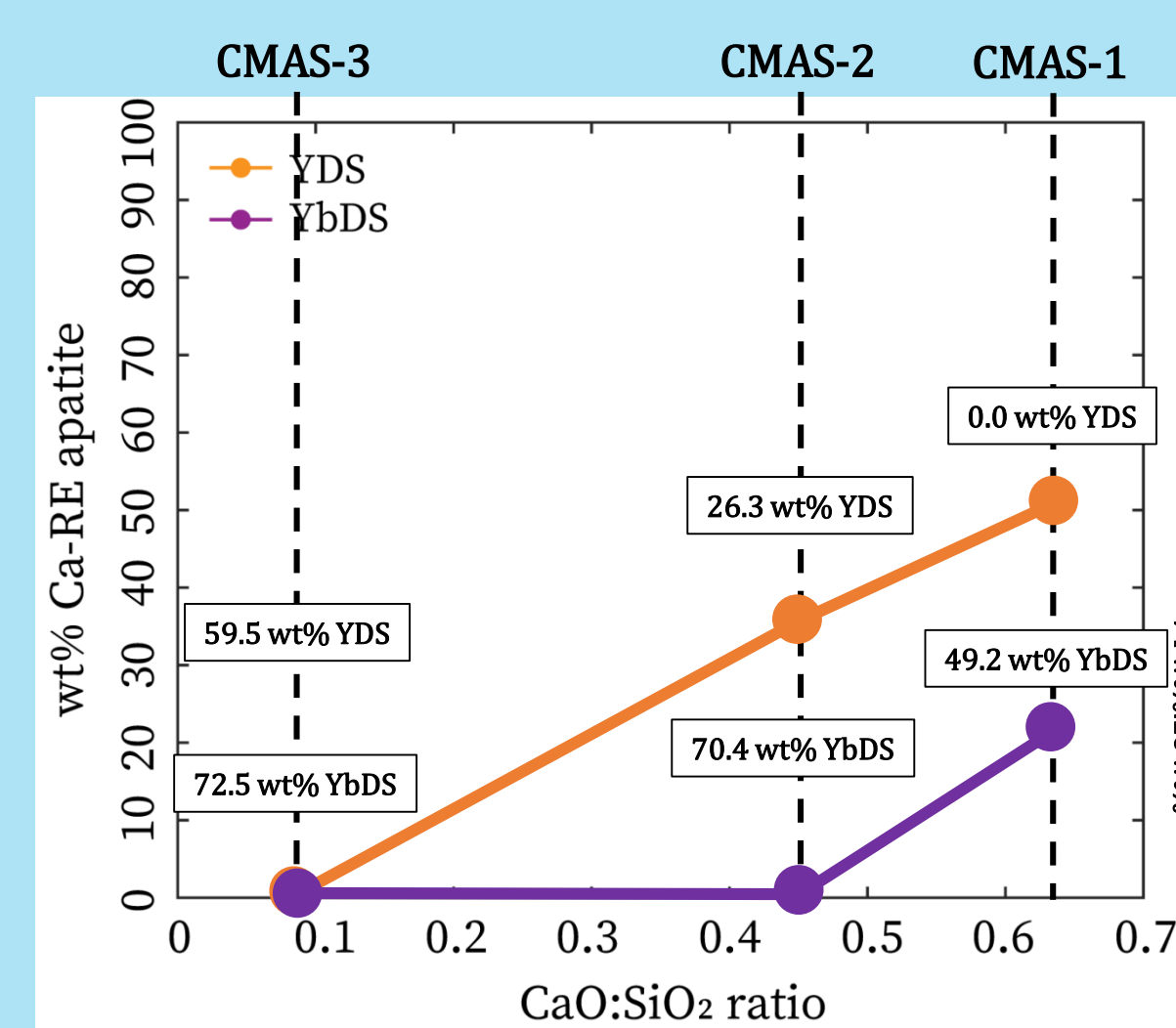
SEM micrographs of a) CMAS-1 b) CMAS-2, and c) CMAS-3 at 1200°C, 1 hour. d) CMAS-3 at 1300°C, 1 hour e) CMAS-3 at 1400°C, 1 hour. Wo = wollastonite, Ano = anorthite, Åk = akermanite, Di = diopside, Cri = cristobalite, G = residual glass

## Small RE Cations with Large RE Cations make Multifunctional RE<sub>2</sub>Si<sub>2</sub>O<sub>7</sub> Compounds

### High-Temperature Thermochemical Interactions of Molten Silicates with Yb<sub>2</sub>Si<sub>2</sub>O<sub>7</sub> (YbDS) and Y<sub>2</sub>Si<sub>2</sub>O<sub>7</sub> (YDS) Environmental Barrier Coating Materials



Reaction products of RE<sub>2</sub>Si<sub>2</sub>O<sub>7</sub>:CMAS with a) CMAS-1 and b) CMAS-3. The apatite, disilicate and SiO<sub>2</sub> phases are marked as blue, green, and yellow, respectively.



Graph of apatite formation as a function of CaO:SiO<sub>2</sub> ratio and RE cation size

As CaO content in the CMAS compositions decreased, apatite formation decreased, which was attributed to reduced apatite stability for smaller RE cations like Y<sup>3+</sup> and Yb<sup>3+</sup>.

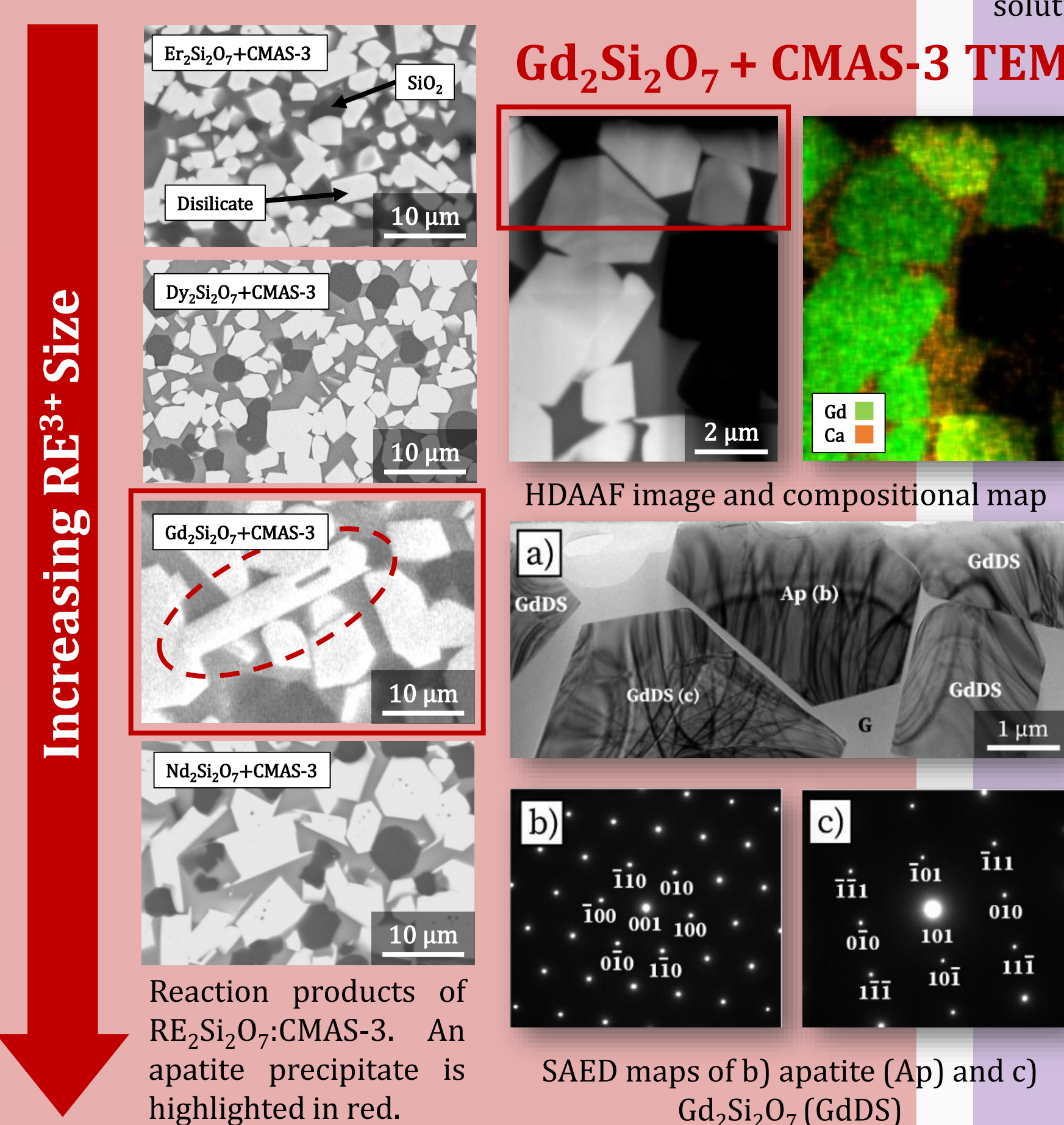
Stokes, J.L., Harder, B.J., Wiesner, V.L., Wolfe, D.E. "High-Temperature Thermochemical Interactions of Molten Silicates with Yb<sub>2</sub>Si<sub>2</sub>O<sub>7</sub> and Y<sub>2</sub>Si<sub>2</sub>O<sub>7</sub> Environmental Barrier Coating Materials" Journal of the European Ceramic Society (2019), doi:10.1016/j.jeurceramsoc.2019.06.051

### Effects of Crystal Structure and Cation Size on Molten Silicate Reactivity with Environmental Barrier Coating Materials

Larger RE disilicates (Ho→La) have not been investigated with CMAS, because materials exhibit vast polymorphism<sup>6</sup> as well as large CTEs<sup>7</sup> that preclude them from EBC use. However, the increased stability of apatite with larger RE cations warranted further investigation into mechanisms of crystallization of CMAS compositions with these materials.

Gd<sup>3+</sup> is the optimal cation size for which apatite formation is favored.

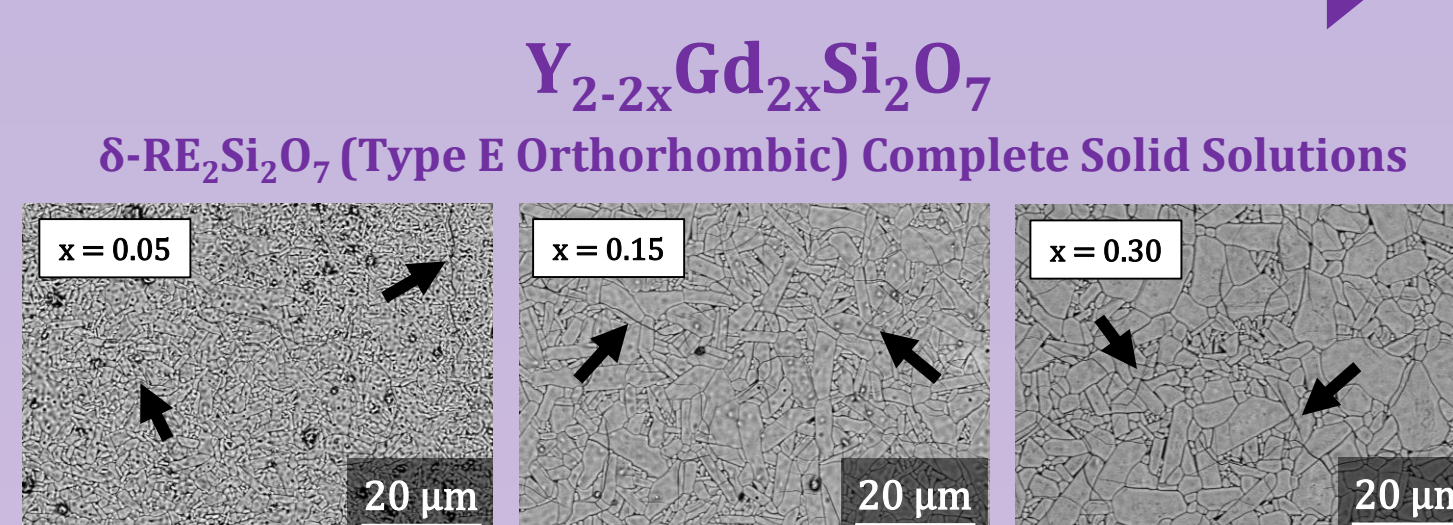
If the cation is too large, there is the risk of higher liquid formation over crystallization.



Stokes, J.L., Harder, B.J., Wiesner, V.L., Wolfe, D.E. "Effects of Crystal Structure and Cation Size on Molten Silicate Reactivity with Environmental Barrier Coating Materials" Journal of the American Ceramic Society (2019), Accepted for Publication

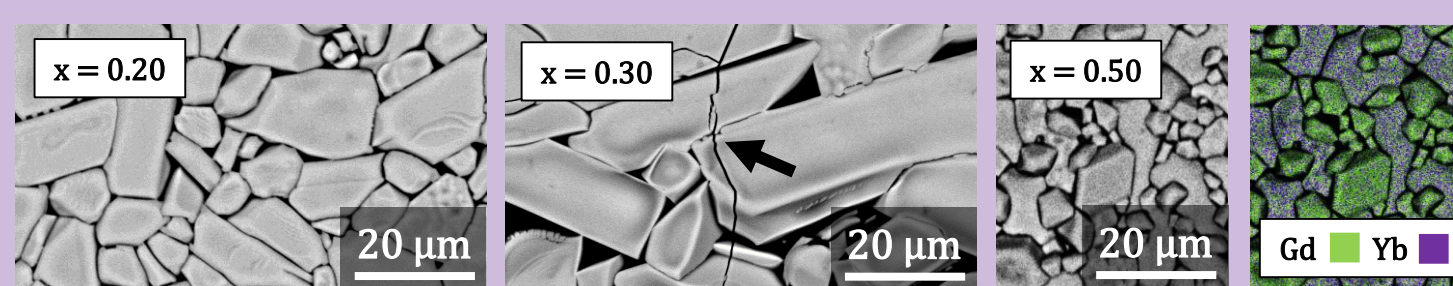
### Solid Solutions in the Yb<sub>2-2x</sub>Gd<sub>2x</sub>Si<sub>2</sub>O<sub>7</sub> and Y<sub>2</sub>Si<sub>2</sub>O<sub>7</sub>-Gd<sub>2</sub>Si<sub>2</sub>O<sub>7</sub> Systems: Phase Transformations and Structure-Property Relationships

#### Increasing Gd<sub>2</sub>Si<sub>2</sub>O<sub>7</sub> Content



SEM micrographs of grain morphologies of Y<sub>2-2x</sub>Gd<sub>2x</sub>Si<sub>2</sub>O<sub>7</sub> and solid solutions. The arrows highlight transgranular cracking. There is an increase in grain growth with increasing GdDS content, which is indicative of an increase in sintering behavior.

#### Yb<sub>2-2x</sub>Gd<sub>2x</sub>Si<sub>2</sub>O<sub>7</sub>



SEM micrographs of grain morphologies of Yb<sub>2-2x</sub>Gd<sub>2x</sub>Si<sub>2</sub>O<sub>7</sub> solid solutions. The arrows highlight transgranular cracking.

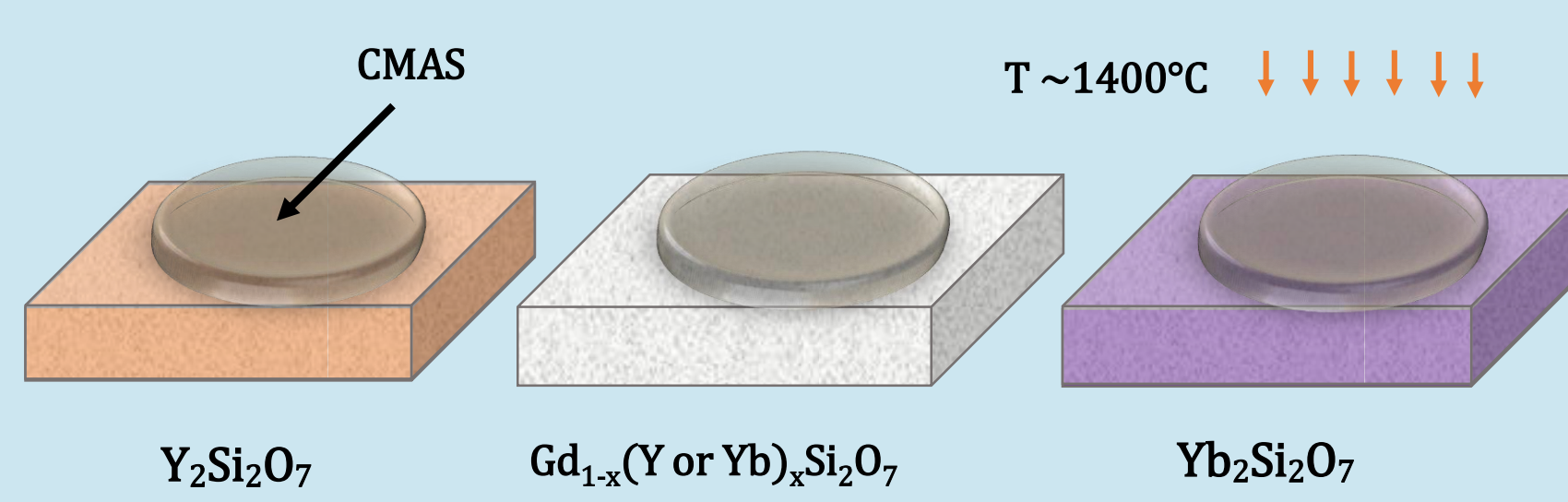
	Lattice	S.G.	CTE
β-RE <sub>2</sub> Si <sub>2</sub> O <sub>7</sub>	Mon	C2/m	~4.0
γ-RE <sub>2</sub> Si <sub>2</sub> O <sub>7</sub>	Mon	P2 <sub>1</sub> /c	~4-4.5
δ-RE <sub>2</sub> Si <sub>2</sub> O <sub>7</sub>	Ortho	Pna2 <sub>1</sub>	~7-9

While Y<sub>2-2x</sub>Gd<sub>2x</sub>Si<sub>2</sub>O<sub>7</sub> form a complete solid solution, the Yb<sub>2-2x</sub>Gd<sub>2x</sub>Si<sub>2</sub>O<sub>7</sub> system exhibits phase transformations and results suggest varying solubility limits of GdDS within certain crystal structures. Important thermal properties related to EBC implementation, such as melting temperature and coefficient of thermal expansion (CTE), will be evaluated as a function of GdDS content.

Stokes, J.L., Harder, B.J., Wiesner, V.L., Wolfe, D.E. "Solid Solutions in the Yb<sub>2</sub>Si<sub>2</sub>O<sub>7</sub>-Gd<sub>2</sub>Si<sub>2</sub>O<sub>7</sub> and Y<sub>2</sub>Si<sub>2</sub>O<sub>7</sub>-Gd<sub>2</sub>Si<sub>2</sub>O<sub>7</sub> Systems: Phase Transformations and Structure-Property Relationships" In Preparation

## Future Work - Environmental Testing

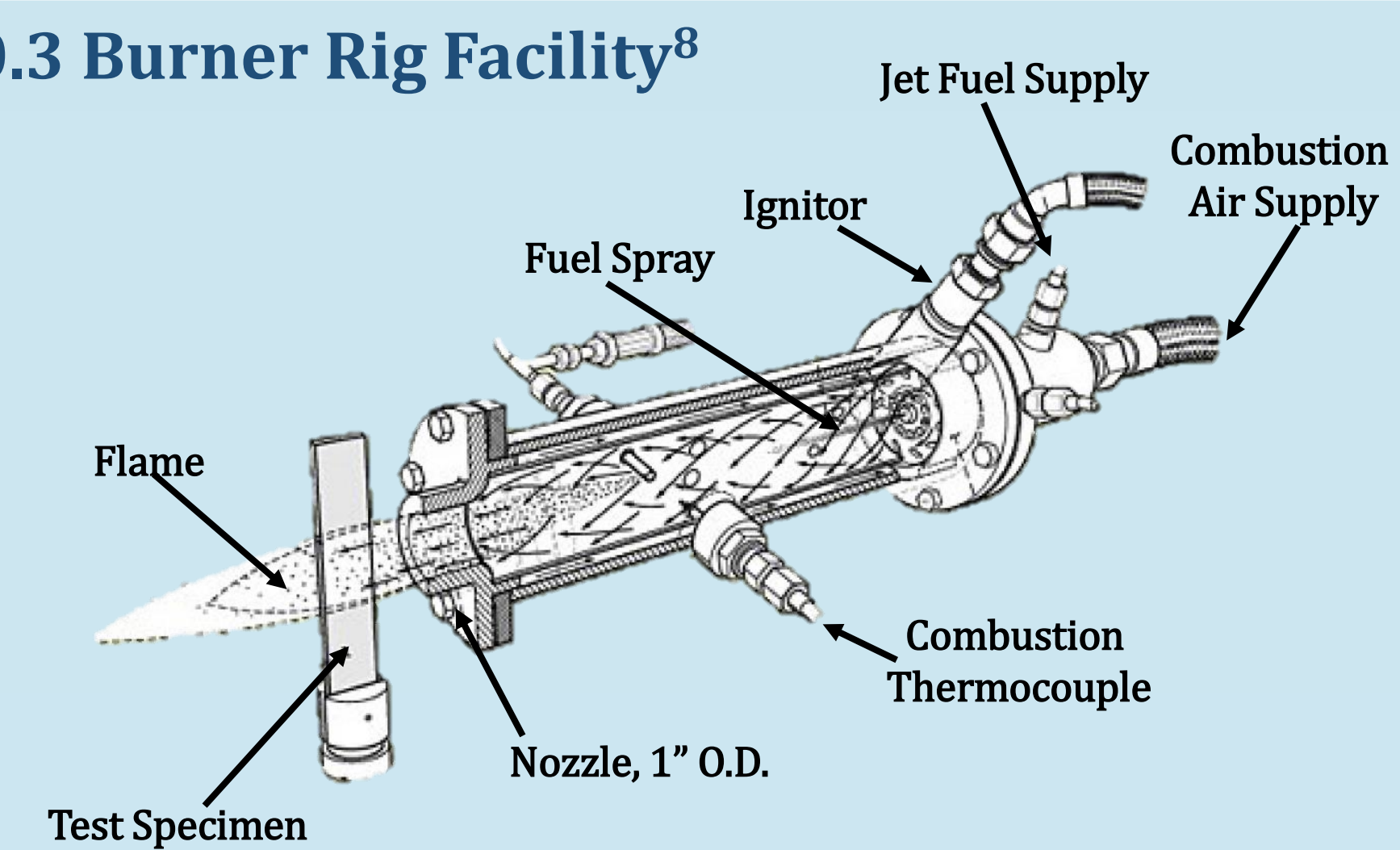
### Furnace Heat Treatment Diffusion Couples



CMAS infiltration rates and depth into doped pellet samples will be investigated and compared to baseline monolithic Y<sub>2</sub>Si<sub>2</sub>O<sub>7</sub> and Yb<sub>2</sub>Si<sub>2</sub>O<sub>7</sub> samples.

### Mach 0.3 Burner Rig Facility<sup>8</sup>

This facility can test materials and components up to ~1375°C in corrosive and oxidative environments. The effects of high temperature, high gas velocity and thermal cycling on CMAS infiltration and corrosion of the doped disilicate coatings can also be determined.



## Conclusions

EBCs are used to protect SiC-based CMCs from high temperature corrosion and oxidation in gas turbine engine systems. However, these materials degrade when exposed to calcium-magnesium-aluminum-silicates (CMAS). Continuing studies aim to improve reactivity of Y<sub>2</sub>Si<sub>2</sub>O<sub>7</sub> and Yb<sub>2</sub>Si<sub>2</sub>O<sub>7</sub> with CMAS particulates via doping of Gd<sub>2</sub>Si<sub>2</sub>O<sub>7</sub>. These studies involve reacting Gd<sub>2</sub>Si<sub>2</sub>O<sub>7</sub> with CMAS and evaluating the thermodynamic equilibria of this material into the Y<sub>2</sub>Si<sub>2</sub>O<sub>7</sub> and Yb<sub>2</sub>Si<sub>2</sub>O<sub>7</sub> crystal structures. The viability of doped coatings to mitigate CMAS damage will be evaluated by diffusion studies and possible environmental testing in a burner rig. These investigations will contribute to the development of new coatings to mitigate CMAS attack, improving the durability of next-generation aircraft engines.

## Acknowledgements and References

This work was supported under the NASA Aeronautics Scholarship and Advanced STEM Training and Research (AS&ASTAR) Graduate Fellowship and the NASA Pathways Intern Employment Program (IEP).

- [1] Krämer S, Yang J, Levi CG. Infiltration-inhibiting reaction of gadolinium zirconate thermal barrier coatings with CMAS melts. *J Am Ceram Soc.* 2008;91(2):576-83.
- [2] Felsche J. The crystal chemistry of the rare-earth silicates. In: *Rare Earths Structure and Bonding*. Springer; 1973. p. 99-197.
- [3] Osborn, E. F., DeVries, R. C., Gee, K. H. & Kraner, H. M. Optimum composition of blast furnace slag as deduced from liquidus data for the quaternary system CaO-MgO-Al<sub>2</sub>O<sub>3</sub>-SiO<sub>2</sub>. *JOM* 6, 33-45 (1954).
- [4] Borom, M. P., Johnson, C. A. & Peluso, L. A. Role of environmental deposits and operating surface temperature in spallation of air plasma sprayed thermal barrier coatings. *Surf. Coatings Technol.* 86-87, 116-126 (1996).
- [5] N.P. Bansal, S.R. Choi, Properties of CMAS glass from desert sand, *Ceram. Int.* 41 (2015) 3901-3909.
- [6] Felsche J. Polymorphism and crystal data of the rare-earth disilicates of type RE<sub>2</sub>Si<sub>2</sub>O<sub>7</sub>. *J Less-Common Met.* 1970;21(1); 1-14.
- [7] Fernández-Carrión, A. J., Allix, M. & Becerro, A. I. Thermal expansion of rare-earth pyrosilicates. *J. Am. Ceram. Soc.* 96, 2298-2305 (2013).
- [8] Fox, D. S. et al. Mach 0.3 Burner Rig Facility at the NASA Glenn Materials Research Laboratory. *NASA/TM-2011-216986* (2011).